

Institut für Regelungs- und Automatisierungstechnik  
**Graz University of Technology**

# Sliding Mode Control: Basic Theory, Advances and Applications

*Elio USAI*

*eusai@diee.unica.it*



**Dept of Electrical and Electronic Eng.**  
***University of Cagliari***

# Lecture 5

---

## Applications of 2<sup>nd</sup> Order Sliding Mode Control to Mechanical Systems

- Simulation of constrained Lagrangian systems
- Overhead crane control
- Contact force regulation in High-Speed train pantographs

# L5 – Simulation of DAE systems

---

Differential Algebraic Equations are often used to model constrained Lagrange-Hamiltonian systems

$$\begin{cases} \mathbf{M}(\mathbf{q})\ddot{\mathbf{q}} + \mathbf{C}(\mathbf{q}, \dot{\mathbf{q}})\dot{\mathbf{q}} + \mathbf{g}(\mathbf{q}) + \mathbf{k}(\mathbf{q}) = \boldsymbol{\tau} + [\mathbf{J}_q^\Phi(\mathbf{q})]^\top \boldsymbol{\lambda} \\ \boldsymbol{\Phi}(\mathbf{q}) = \mathbf{0} \end{cases}$$

$\mathbf{q} \in \mathbb{R}^n$  is the vector of generalized Lagrange position coordinates

$\boldsymbol{\tau} \in \mathbb{R}^n$  is the vector of the generalized input forces

$\boldsymbol{\lambda} \in \mathbb{R}^m$  is the vector of the Lagrange multipliers (constraint reaction forces)

$[\mathbf{J}_q^\Phi]^\top \boldsymbol{\lambda}$  is the vector of the generalized reaction forces

$\mathbf{M}$  is inertia matrix

$\mathbf{C}$  term takes into account for the Coriolis and inertial forces

$\mathbf{g}$  represents the gravitational (potential) forces

$\mathbf{k}$  represents the elastic forces

$\boldsymbol{\Phi}: \mathbb{R}^n \rightarrow \mathbb{R}^m$  is a smooth function representing the constraint

# L5 – Simulation of DAE systems

---

Differentiating twice the constraint function the Lagrange multipliers appears (the relative degree between the constraint and the Lagrange multipliers is 2)

$$\ddot{\Phi}(\mathbf{q}) = \mathbf{f}(\mathbf{q}, \dot{\mathbf{q}}, \boldsymbol{\tau}) + \mathbf{J}_q^\Phi(\mathbf{q}) \cdot \mathbf{M}^{-1}(\mathbf{q}) [\mathbf{J}_q^\Phi(\mathbf{q})]^\top \cdot \boldsymbol{\lambda}$$

The matrix left multiplying the Lagrange multipliers is definite positive by construction and by the properties of Lagrange-Hamiltonian systems

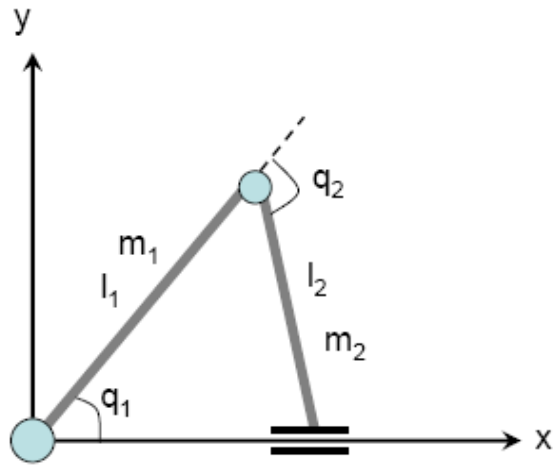
The constraint function can be considered to defining a sliding variable to be constrained to zero by means of the “control”  $\boldsymbol{\lambda}$

$$\mathbf{s} = \dot{\Phi}(\mathbf{q}) + c\Phi(\mathbf{q}) \quad \text{Classic 1-SMC+LP filter or Super-Twisting 2-SMC}$$

$$\mathbf{s} = \Phi(\mathbf{q}) \quad \text{2-SMC+LP filter}$$

# L5 – Simulation of DAE systems

Example: Constrained planar manipulator



$$\mathbf{M}(\mathbf{q}) = \begin{bmatrix} 0.83 + 0.5\cos(q_2) & 0.16 + 0.25\cos(q_2) \\ 0.16 + 0.25\cos(q_2) & 0.16 \end{bmatrix},$$

$$\mathbf{C}(\mathbf{q}, \dot{\mathbf{q}}) = \begin{bmatrix} -1.01\dot{q}_2\sin(q_2) & 1.01(\dot{q}_1 + \dot{q}_2)\sin(q_2) \\ 1.01\dot{q}_1\sin(q_2) & 0 \end{bmatrix},$$

$$\mathbf{g}(\mathbf{q}) = \begin{bmatrix} 9.8\cos(q_1) + 2.45\cos(q_1 + q_2) \\ 2.45\cos(q_1 + q_2) \end{bmatrix}, \quad \mathbf{k}(\mathbf{q}) = \begin{bmatrix} 0 \\ 0 \end{bmatrix}.$$

$$\Phi(\mathbf{q}) = l_1 \sin(q_1) + l_2 \sin(q_1 + q_2) = 0$$

The manipulator is forced  
by the unique torque  
applied to the first arm

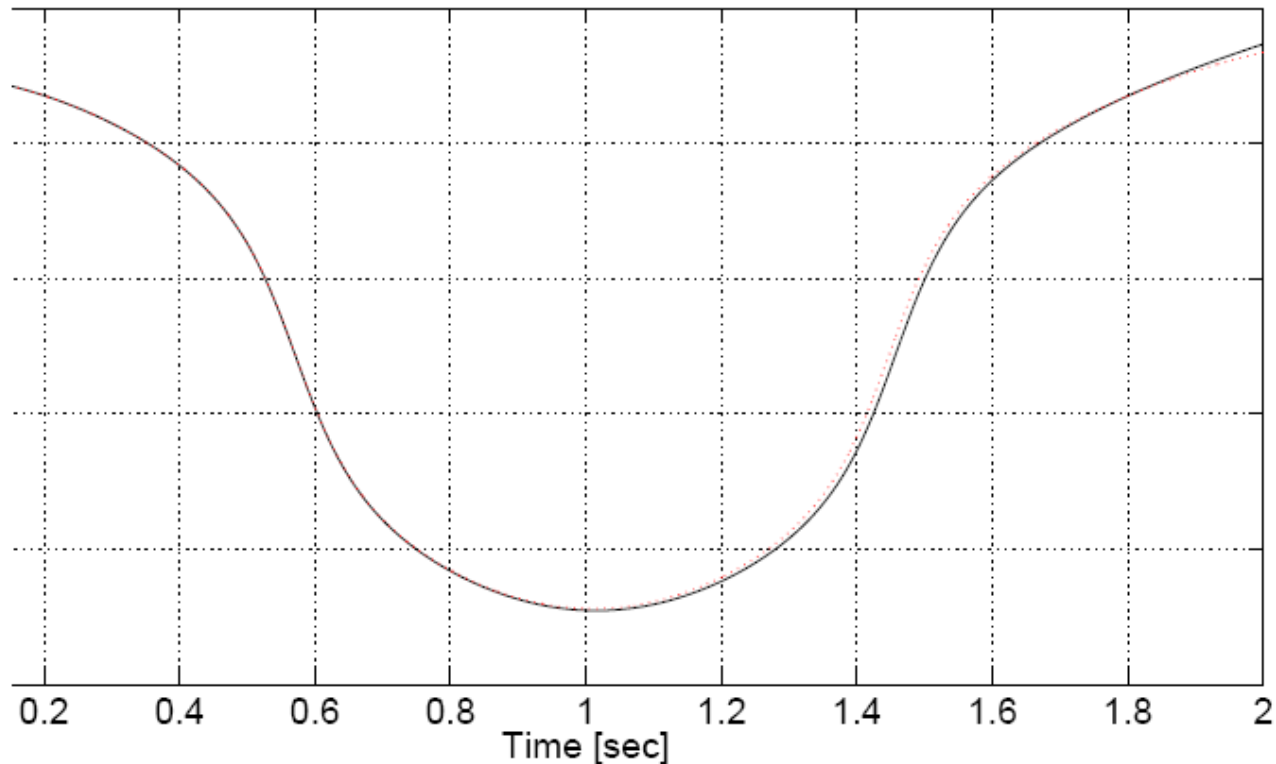
$$\boldsymbol{\tau} = \begin{bmatrix} \sin(t) \\ 0 \end{bmatrix}$$

# L5 – Simulation of DAE systems

---

Example: Constrained planar manipulator ( $T_s=10^{-5}$  s)

Joint coordinate  $q_1$  with first- and second-order SMC approach

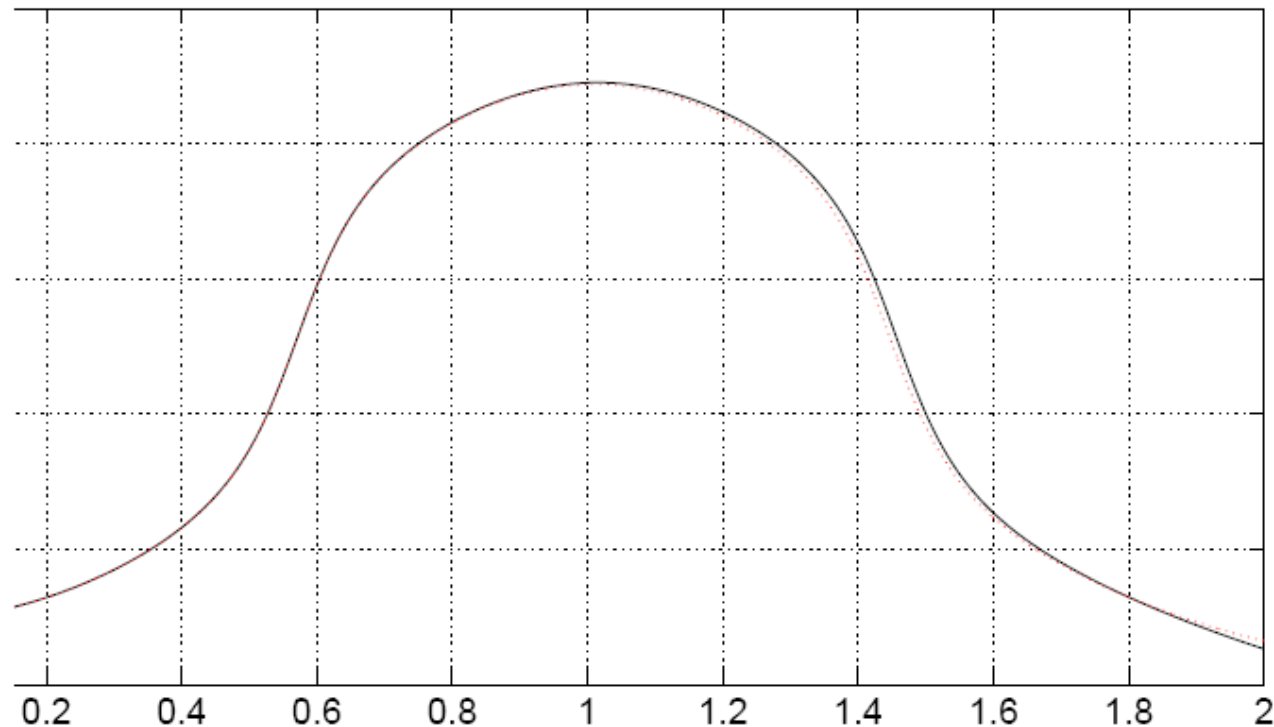


# L5 – Simulation of DAE systems

---

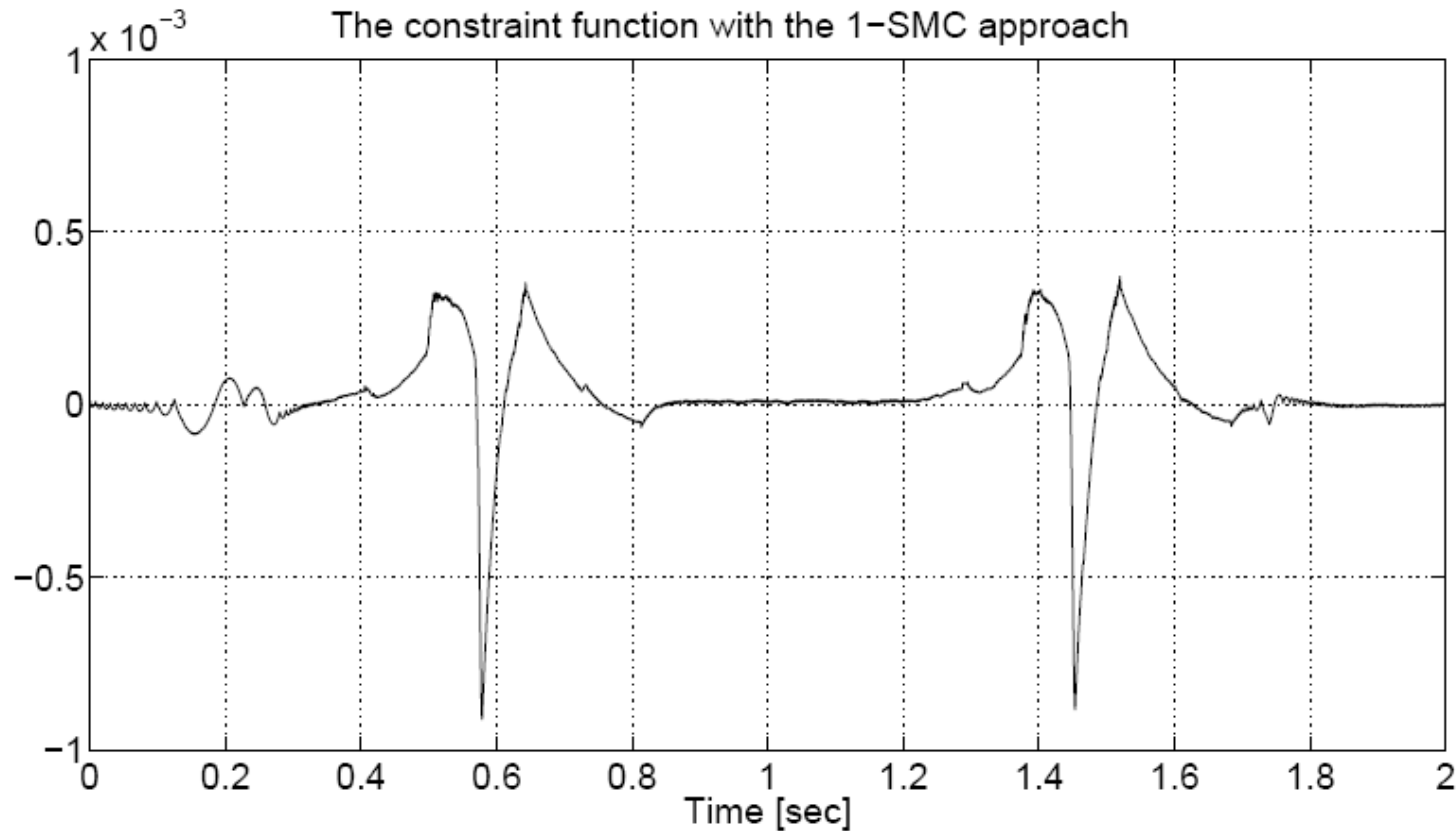
Example: Constrained planar manipulator ( $T_s=10^{-5}$  s)

Joint coordinate  $q_2$  with first- and second-order SMC approach



# L5 – Simulation of DAE systems

Example: Constrained planar manipulator ( $T_s=10^{-5}$  s)

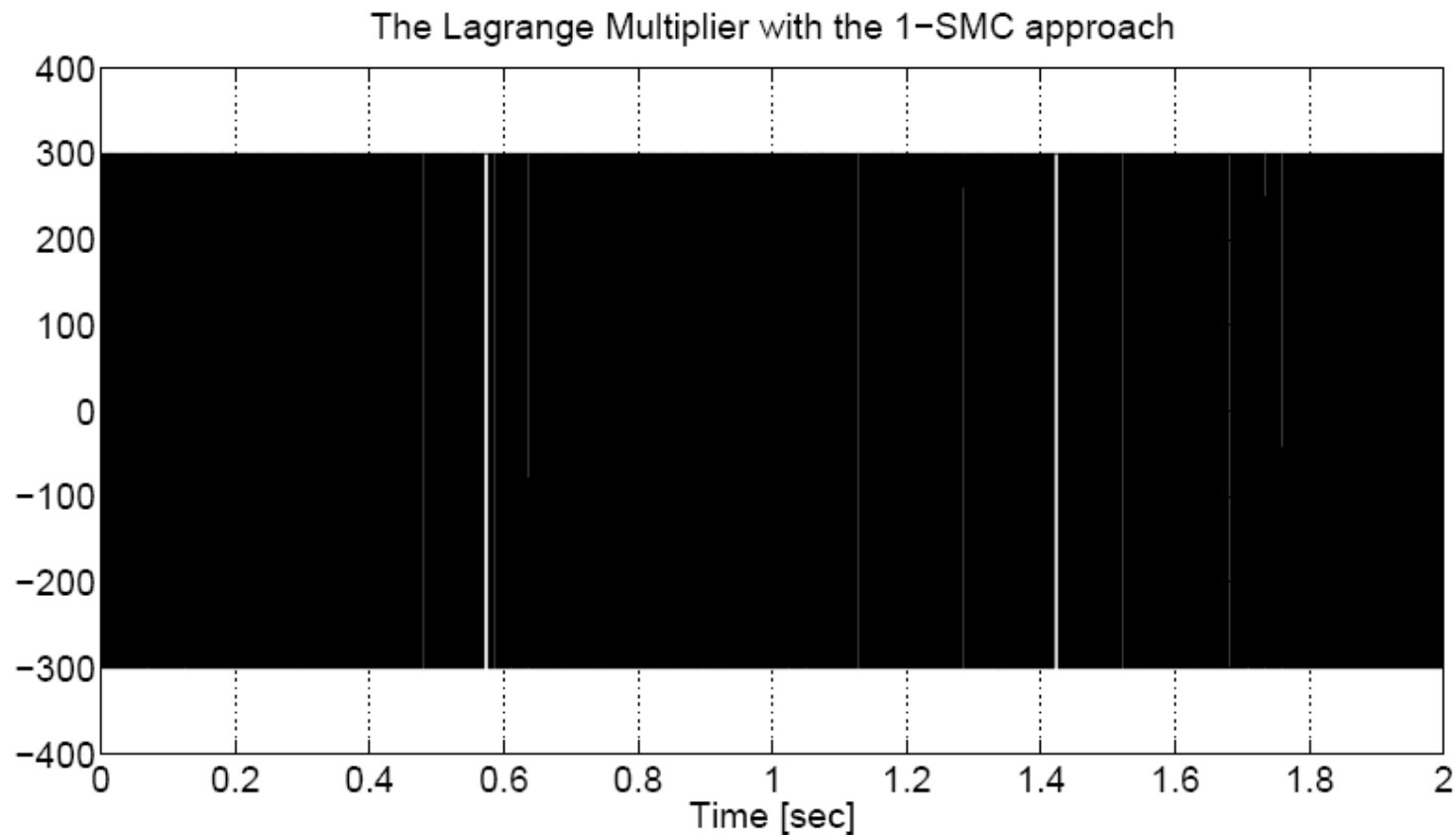


The magnitude of the switching control is set to  $U=300$

# L5 – Simulation of DAE systems

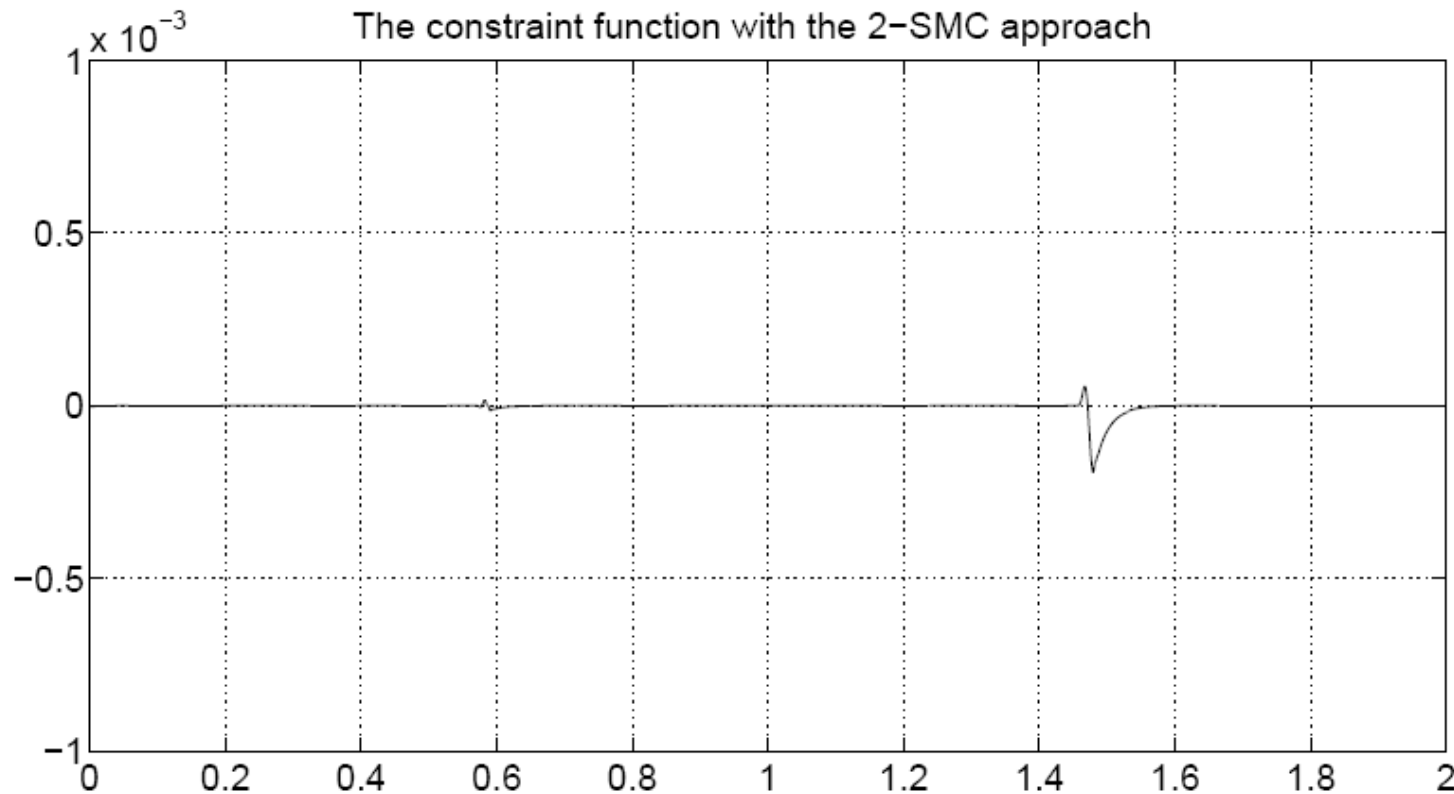
---

Example: Constrained planar manipulator ( $T_s=10^{-5}$  s)



# L5 – Simulation of DAE systems

Example: Constrained planar manipulator ( $T_s=10^{-5}$  s)



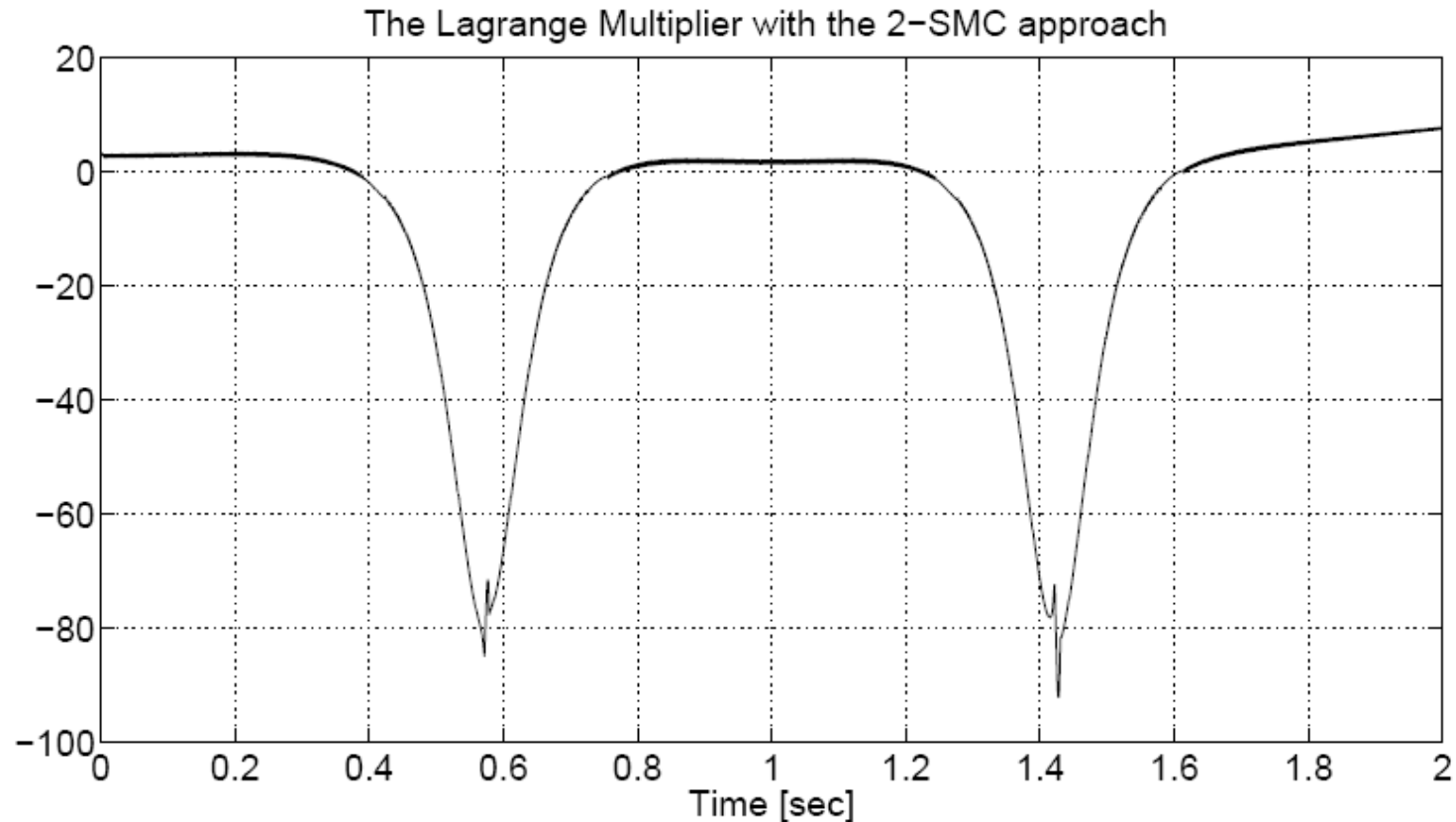
The magnitude of the continuous term is  $\lambda=10$

The magnitude of the switching term is  $\alpha=100$

# L5 – Simulation of DAE systems

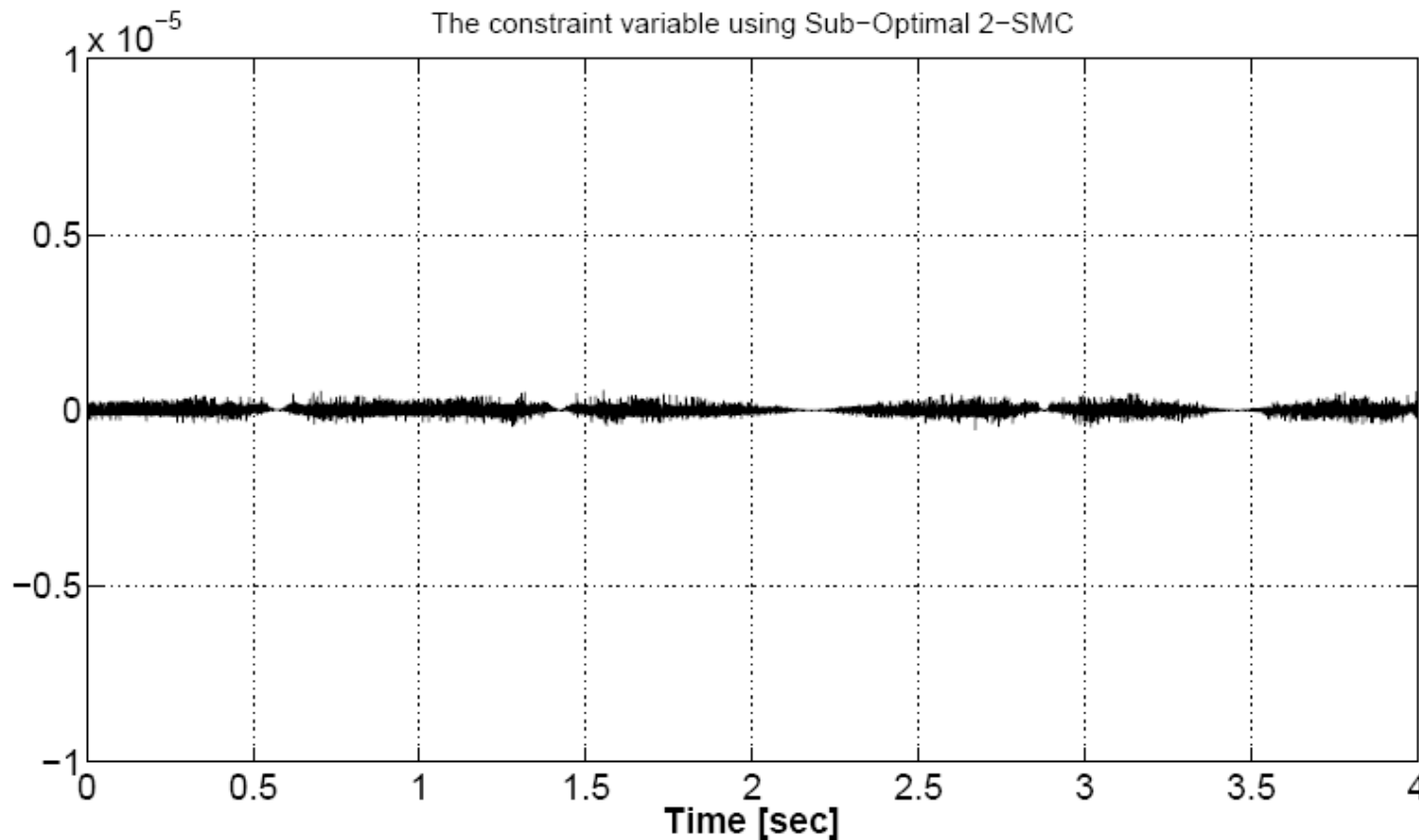
---

Example: Constrained planar manipulator ( $T_s=10^{-5}$  s)



# L5 – Simulation of DAE systems

Example: Constrained planar manipulator ( $T_s=10^{-5}$  s)



The magnitude of the control is  $U=300$

The anticipation parameter is  $\beta=0.8$

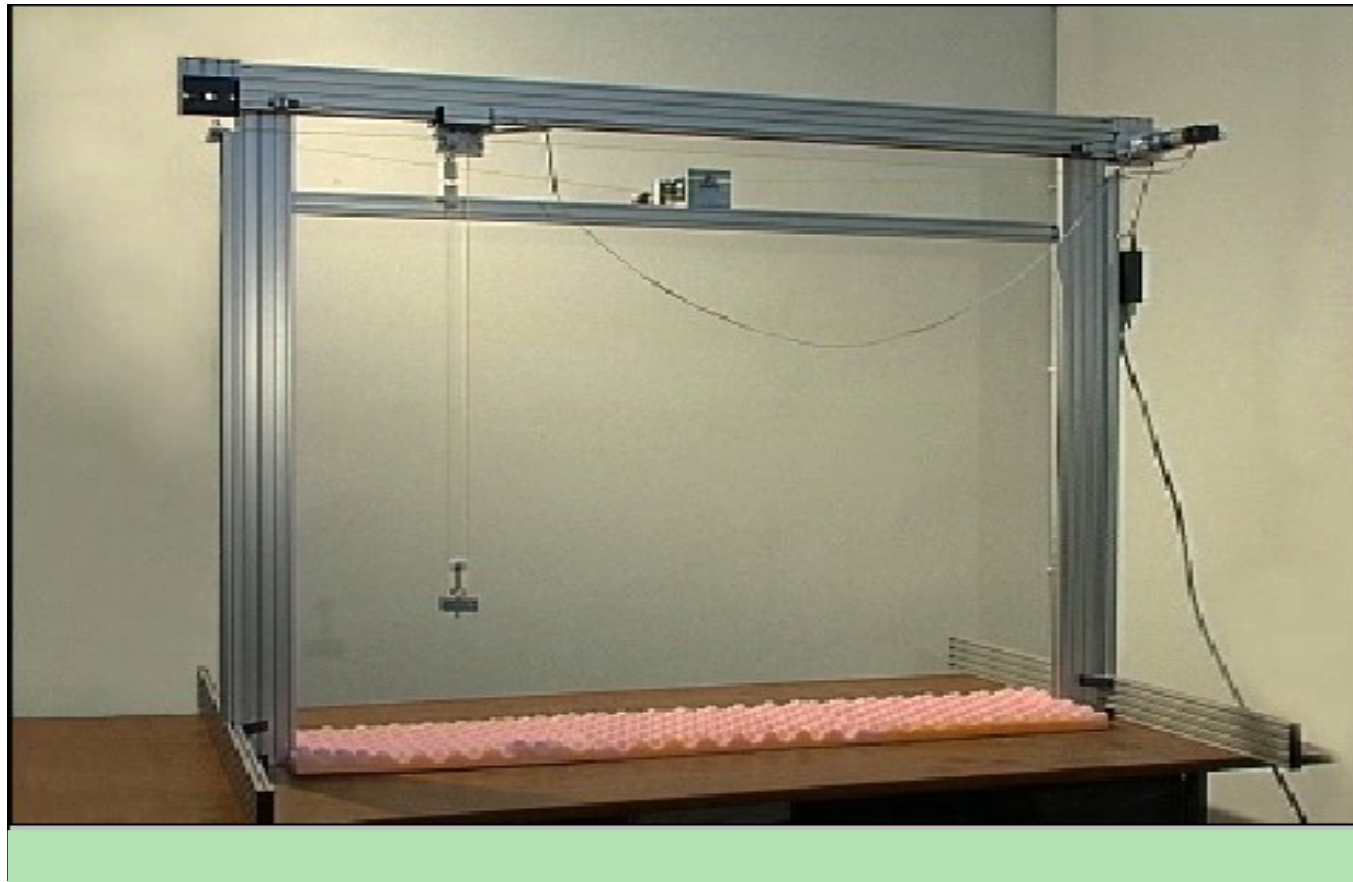
Since the accuracy is very high the plot of the Lagrange multiplier clearly shows two singular ( $\infty$ ) points

# L5 – Overhead crane control

---

Overhead cranes are used to move heavy loads, and for shipping procedures of containers

Laboratory-sized prototype



# L5 – Overhead crane control

## Overhead Crane Model

### Mechanical subsystem

$$A_1 \ddot{x}_t + B_1 (\ddot{l} \sin \varphi + l \ddot{\varphi} \cos \varphi + 2 \dot{l} \dot{\varphi} \cos \varphi - l \dot{\varphi}^2 \sin \varphi) = T_1$$

$$B_2 \ddot{x}_t \sin \varphi + A_2 \ddot{l} - B_2 l (\dot{\varphi}^2 + g \cos \varphi) = T_2$$

$$\ddot{x}_t \cos \varphi + l \ddot{\varphi} + 2 \dot{l} \dot{\varphi} + g \sin \varphi = 0$$

$x_t$ : trolley position

$l$ : rope length

$\varphi$ : load oscillation angle

$T_1, T_2$ : trolley and hoisting torques

### Electrical torque actuators: DC Motors)

$$L \dot{\mathbf{T}} + R \mathbf{T} - K \begin{vmatrix} \dot{x}_t \\ \dot{l} \end{vmatrix} = \begin{vmatrix} V_1 \\ V_2 \end{vmatrix}$$

$V_1, V_2$ : motor voltages

# L5 – Overhead crane control

Sliding manifold design

$$\begin{aligned}\sigma_1 &= \dot{x}_t - \dot{x}_t^* + c_x (x_t - x_t^*) - k \varphi \\ \sigma_2 &= \dot{l} - \dot{l}^* + c_y (l - l^*)\end{aligned}$$

The zero-dynamics

$$\begin{aligned}\dot{x}_t &= \dot{x}_t^* - c_x (x_t - x_t^*) + k \varphi \\ \dot{l} &= \dot{l}^* - c_y (l - l^*) \\ \ddot{\varphi} &= -\frac{g}{l} \varphi - \frac{1}{l} [\ddot{x}_t^* - c_x (x_t - x_t^*)] - \frac{k + 2(\dot{l}^* - c_y (l - l^*))}{l} \dot{\varphi}\end{aligned}$$

The sliding dynamics

$$\begin{bmatrix} \ddot{\sigma}_1 \\ \ddot{\sigma}_2 \end{bmatrix} = \begin{bmatrix} f_1(\cdot) \\ f_2(\cdot) \end{bmatrix} + \mathbf{G}(\cdot) \begin{bmatrix} V_1 \\ V_2 \end{bmatrix}$$

$f_i$  are uncertain but bounded

$\mathbf{G}$  is almost diagonal

$V_i$  are the motor supply voltages

# L5 – Overhead crane control

---

## Zero-dynamics stability

### 1. Traveling phase

$$\dot{x}^* = V_0 = \text{const.}$$
$$c_x = 0$$

STABILITY CONDITION

$$k_m \leq k \leq k_M$$

The crane parameters do not affect the above stability condition, which depends only on the desired trajectory

### 2. Arrival phase (neighbor of the destination point $(x_f, y_f)$ )

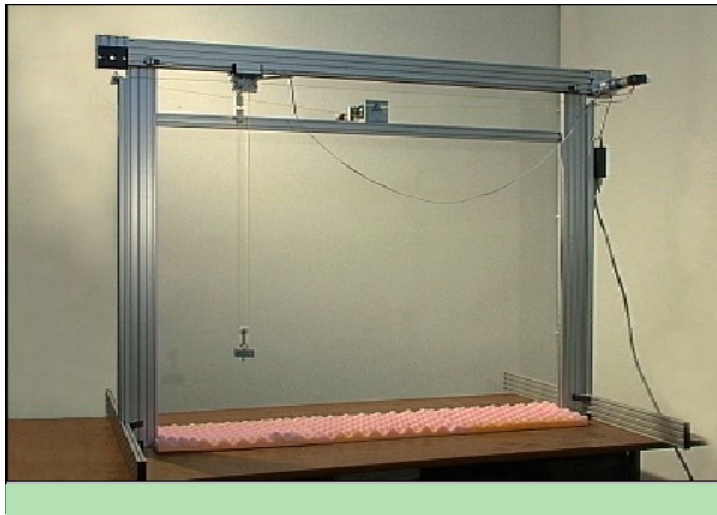
$$x^* = x_f$$
$$y^* = y_f$$
$$\dot{x}^* = \dot{y}^* = 0$$

STABILITY CONDITION

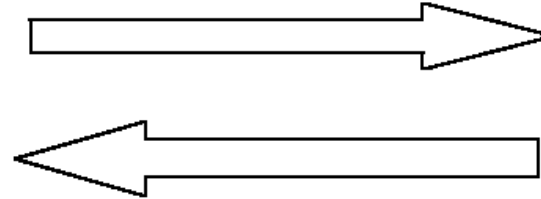
$$0 < k < \frac{g}{c_x}$$

# L5 – Overhead crane control

## Experimental set-up



$x_t, l, \varphi$   
(trolley and hoist motor  
positions and swing angle)



$v_t, v_l$   
(trolley and hoist  
motor voltages)



PC UNIT

2-SM differentiators are implemented for estimating the trolley and rope velocities

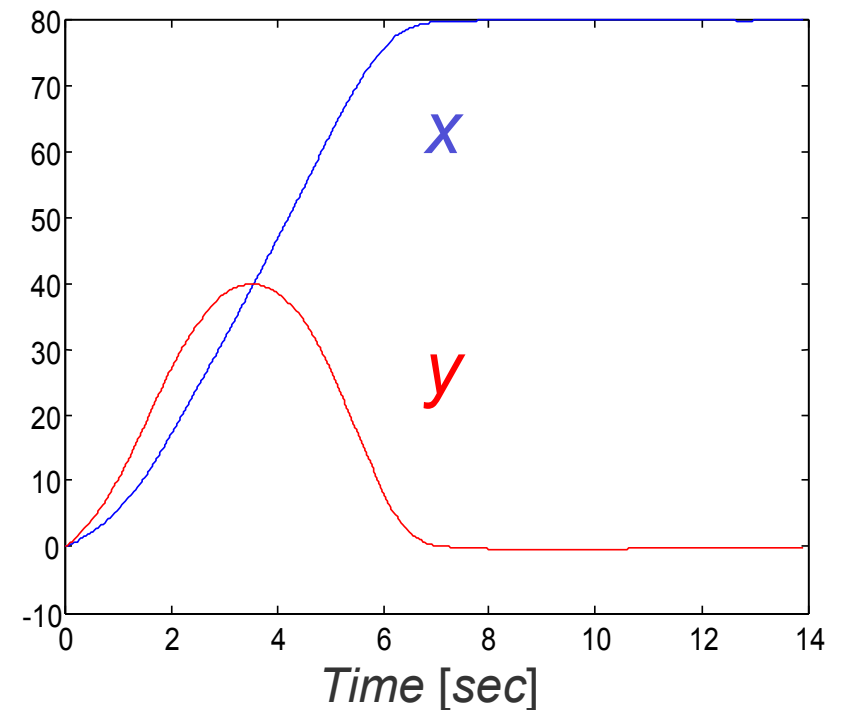
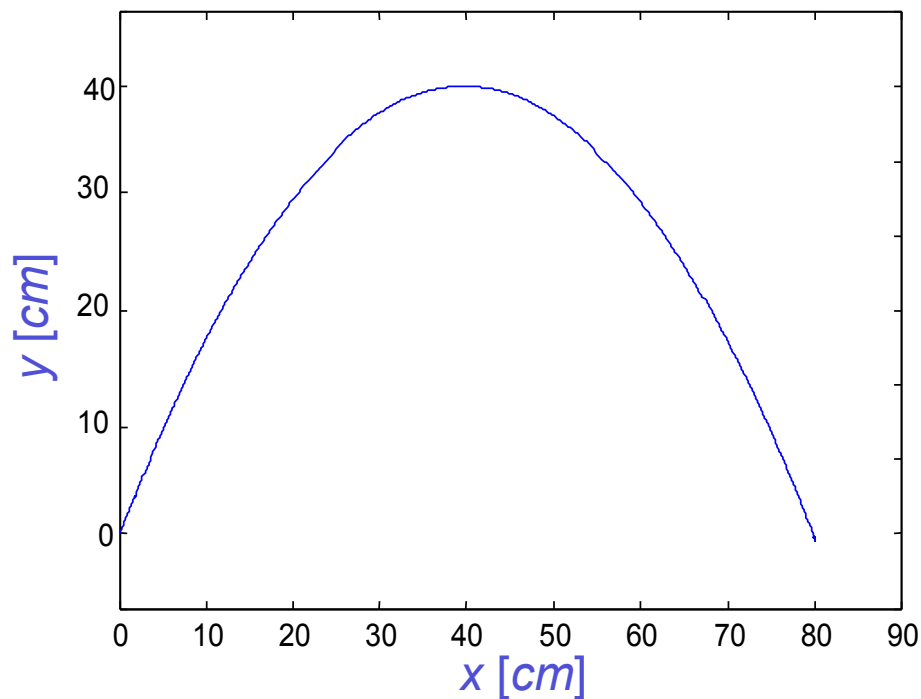
2 instances of the sub-optimal 2-SMC are implemented

Direct discretization of the differentiators and controllers with  $T_s = 2ms$  is implemented

# L5 – Overhead crane control

## Experiment 1 – simple traveling and hoisting

### The actual and reference load coordinates



Traveling velocity of the trolley is 15 m/s

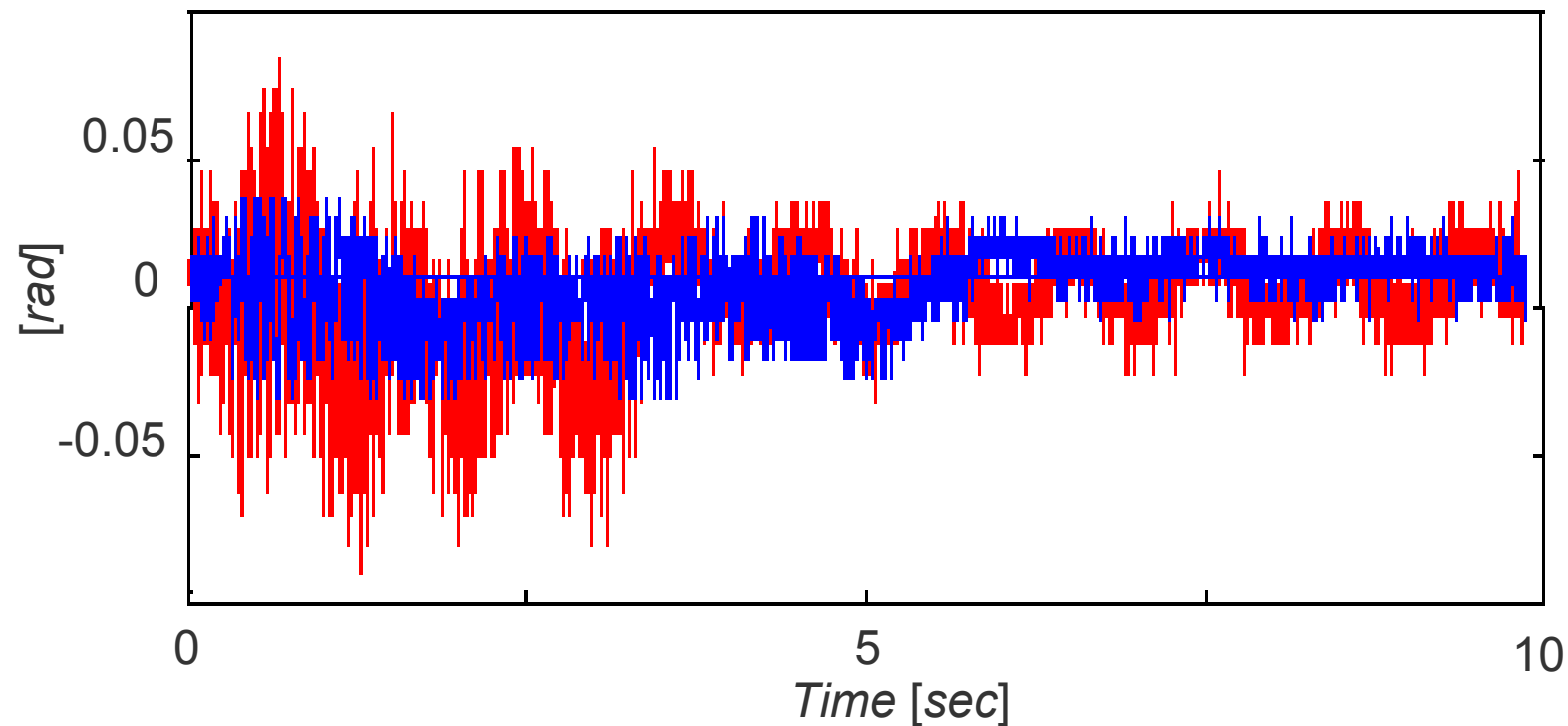
# L5 – Overhead crane control

Experiment 1 – simple traveling and hoisting

The load swing

$k=0$

$k=80$

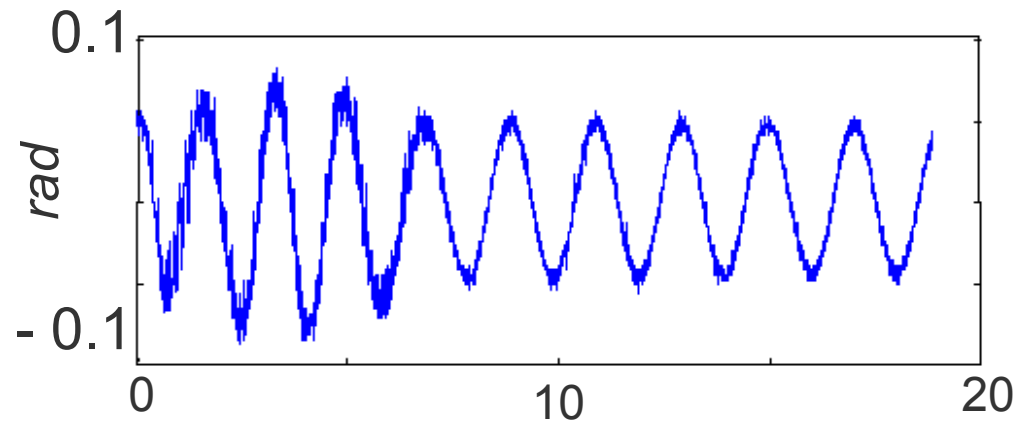


Traveling velocity of the trolley is 15 m/s

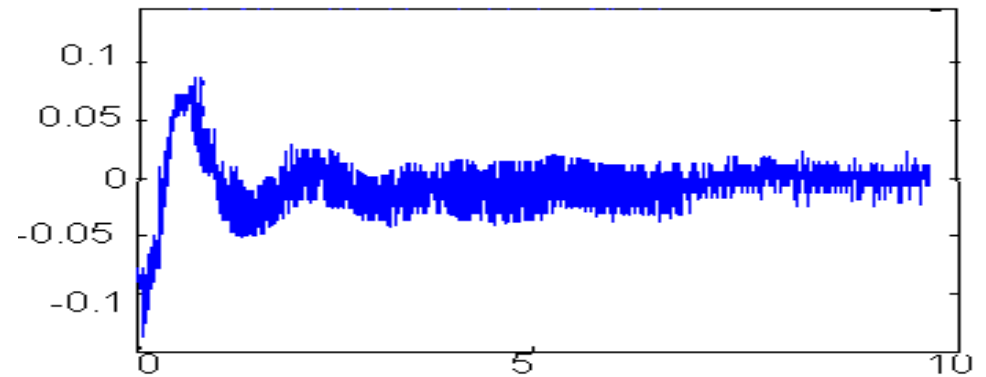
# L5 – Overhead crane control

Experiment 2 – traveling and hoisting with initial oscillation

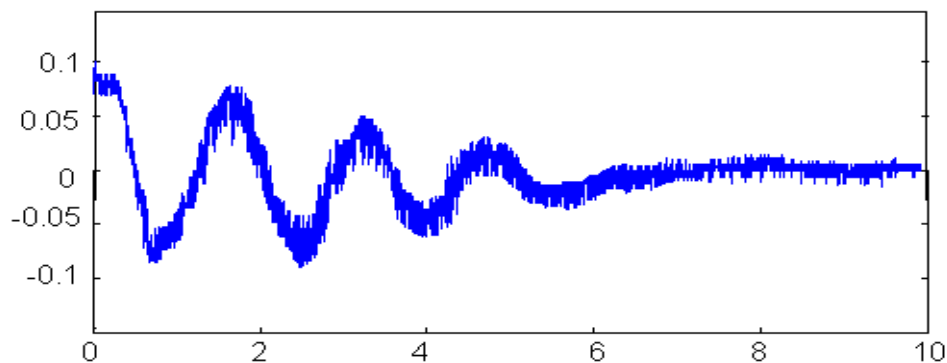
$k=0$  (no swing control)



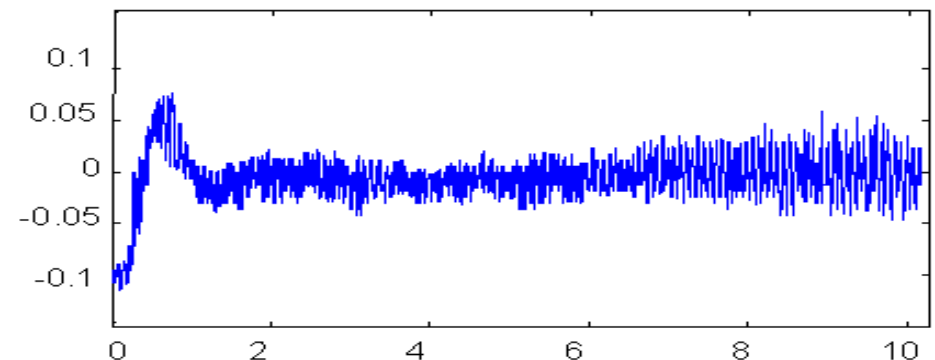
$k=360$



$k=80$



$k=640$  (unstable oscillations)



# L5 – Overhead crane control - Video



*Department of Electrical and Electronic Engineering  
University of Cagliari, Piazza D'Armi  
09123 Cagliari, Italy*

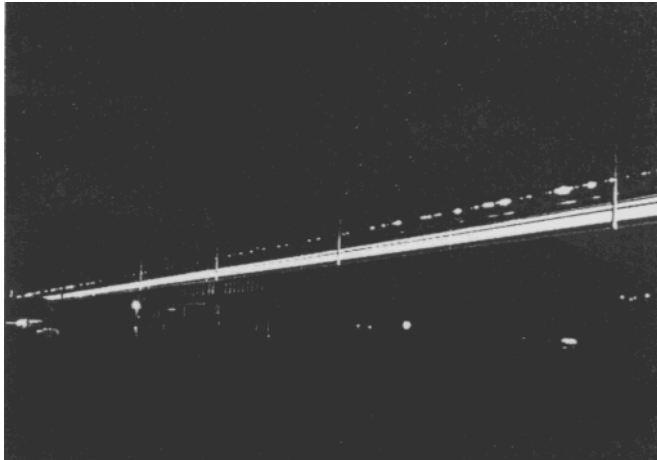
*+39 07067.55895      Fax: +39 07067.55900*

## Overhead crane control by second order sliding modes

### Experimental results

# L5 – Contact Force Regulation

---



Pantograph-catenary interaction causes oscillations due to the moving force on the contact wire.

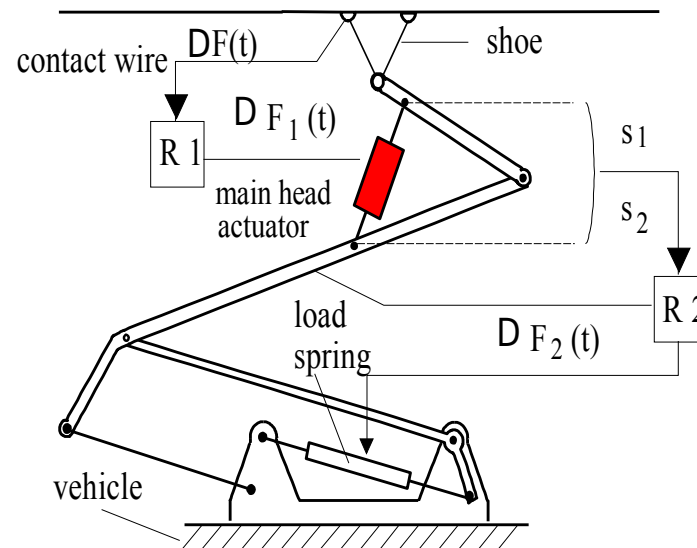
Contact force variations cause:

- Loss of contact and electric arcs
- Wire and shoe wearing

**Possible solutions:**

- Increase the tension of the contact wire
- More rigid catenary systems
- Reduce the pantograph weight
- Use of active pantographs

# L5 – Contact Force Regulation



## Two options for actuator location

Head (upper frame) actuated

*minor control effort*

*difficulties in positioning*

Lower frame actuated

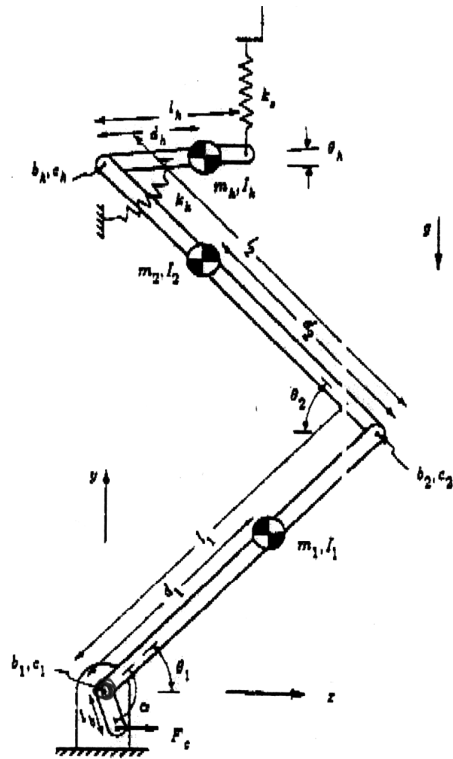
*major control effort*

*simple positioning*

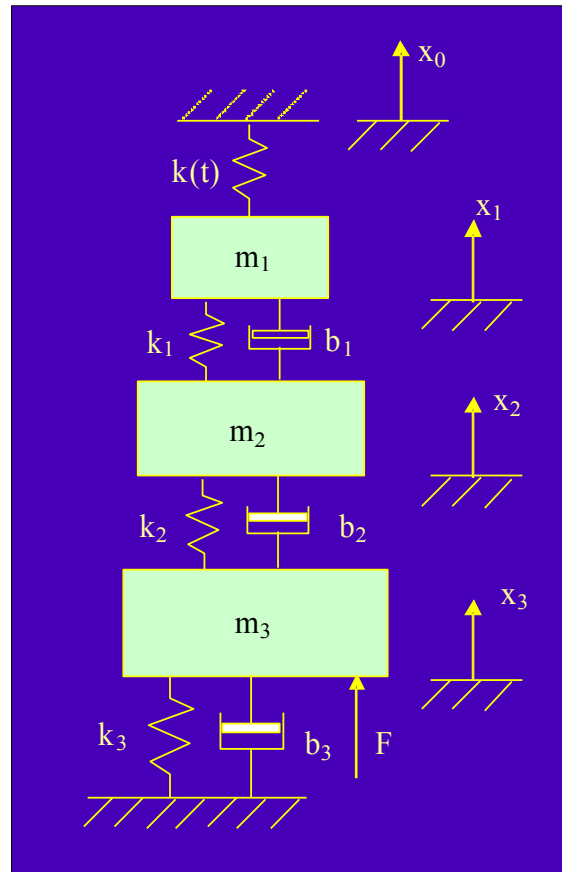
**Low-cost changes to passive pantographs: wire actuators**

# L5 – Contact Force Regulation

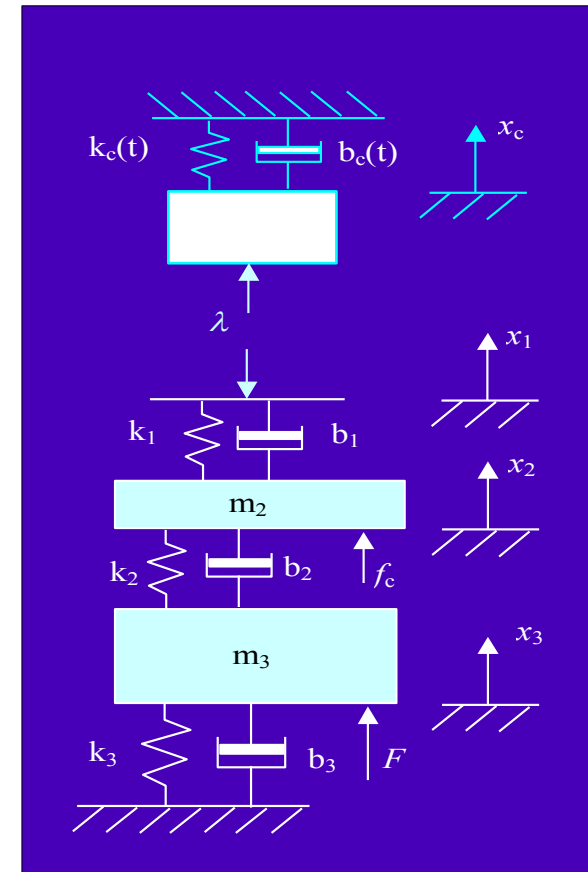
## Pantograph models



nonlinear  
3 d.o.f.



linear  
3 d.o.f.



Linear 3DOF  
including loss  
of contact

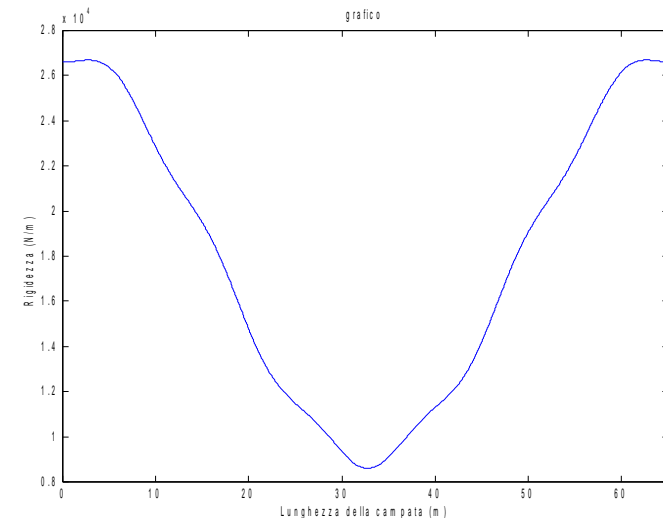
# L5 – Contact Force Regulation

## Pantograph models

$$m_c(x) = m_{c_0} + \sum_{i=1}^p m_{s_i} \cos\left(\frac{2\pi}{L_s} ix\right) + \sum_{i=1}^q m_{p_i} \sin\left(\frac{2\pi}{L_p} ix\right),$$

$$b_c(x) = b_{c_0} + \sum_{i=1}^p b_{s_i} \cos\left(\frac{2\pi}{L_s} ix\right) + \sum_{i=1}^q b_{p_i} \sin\left(\frac{2\pi}{L_p} ix\right),$$

$$k_c(x) = k_{c_0} + \sum_{i=1}^p k_{s_i} \cos\left(\frac{2\pi}{L_s} ix\right) + \sum_{i=1}^q k_{p_i} \sin\left(\frac{2\pi}{L_p} ix\right),$$

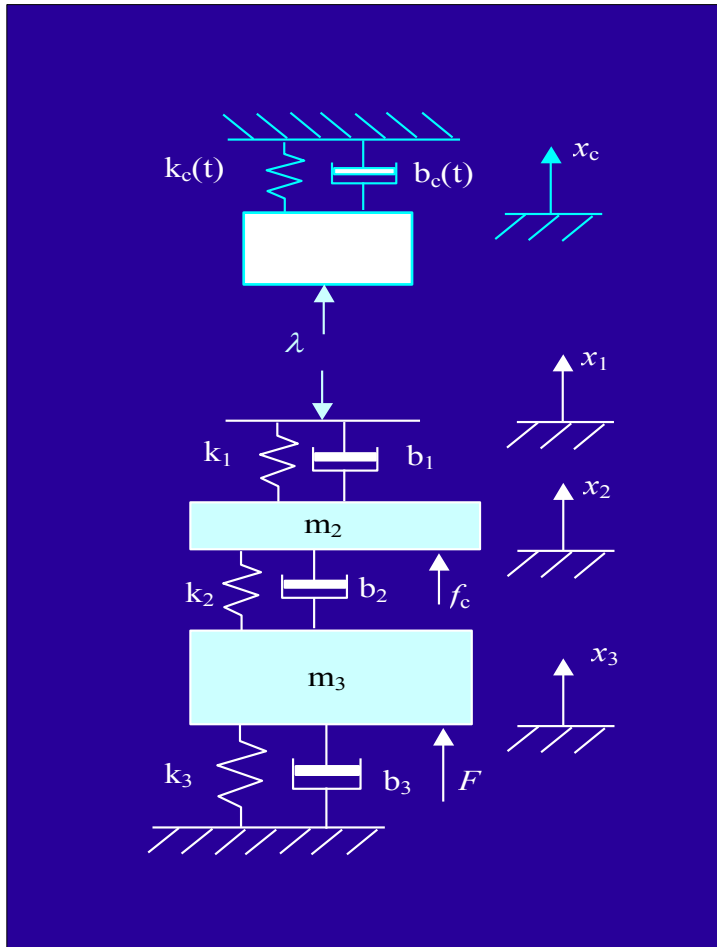


$$k_c(t) = k_{c_0} \left( 1 + \alpha \cos\left(\frac{2\pi v}{L_s} t\right) + \beta \sin\left(\frac{2\pi v}{L_p} t\right) \right)$$

The approximate model of the catenary is reduced to a time varying lumped parameter model depending on the train velocity

# L5 – Contact Force Regulation

Pantograph models without loss of contact



$$\dot{\mathbf{z}}(t) = \mathbf{A}(t)\mathbf{z}(t) + \mathbf{B}\mathbf{f}(t)$$

$$\mathbf{y}(t) = \mathbf{C}\mathbf{z}(t)$$

$$\mathbf{A}(t) = \begin{bmatrix} 0 & 1 & 0 & 0 & 0 & 0 \\ -\frac{k_c(t)+k_1}{m_c(t)} & -\frac{b_c(t)+b_1}{m_c(t)} & \frac{k_1}{m_c(t)} & \frac{b_1}{m_c(t)} & 0 & 0 \\ 0 & 0 & 0 & 1 & 0 & 0 \\ \frac{k_1}{m_2} & \frac{b_1}{m_2} & -\frac{k_1+k_2}{m_2} & -\frac{b_1+b_2}{m_2} & \frac{k_2}{m_2} & \frac{b_2}{m_2} \\ 0 & 0 & 0 & 0 & 0 & 1 \\ 0 & 0 & \frac{k_2}{m_3} & \frac{b_2}{m_3} & -\frac{k_2+k_3}{m_3} & -\frac{b_2+b_3}{m_3} \end{bmatrix}$$

$$\mathbf{B} = \begin{bmatrix} 0 & 0 \\ 0 & 0 \\ 0 & 0 \\ \frac{1}{m_2} & 0 \\ 0 & 0 \\ 0 & \frac{1}{m_3} \end{bmatrix}$$

$$\mathbf{C} = [-k_1 \quad -b_1 \quad k_1 \quad b_1 \quad 0 \quad 0]$$

# L5 – Contact Force Regulation

## Pantograph dynamics

**Dynamics of the wire-type actuators**

$$\ddot{f}_c + 2\zeta_f \omega_{nf} \dot{f}_c + \omega_{nf}^2 f_c = \omega_{nf}^2 K_{af} u_f$$
$$\ddot{F} + 2\zeta_F \omega_{nF} \dot{F} + \omega_{nF}^2 F = \omega_{nF}^2 K_{aF} u_F$$

The sliding variable

$$\sigma = y - y_d \quad y_d = 100N$$

Normal-form dynamics  
considering the upper frame  
actuation

$$\ddot{\sigma}(t) = \varphi(\mathbf{y}(t), \mathbf{w}(t), t) + \gamma \cdot u_f(t),$$
$$\dot{\mathbf{w}}(t) = \boldsymbol{\psi}(\mathbf{y}(t), \mathbf{w}(t), t),$$

Relative degree is three because of the 2<sup>nd</sup> order dynamics of the actuator

The internal dynamics are BIBS stable

# L5 – Contact Force Regulation

---

## Controller design

$$u = -U \operatorname{sgn}(\hat{\sigma} - \beta \hat{\sigma}_{ex})$$

The controller gain is tuned taking into account the nominal dynamics of the system with an additional integrator for anti-chattering purpose, disregarding the actuator dynamics

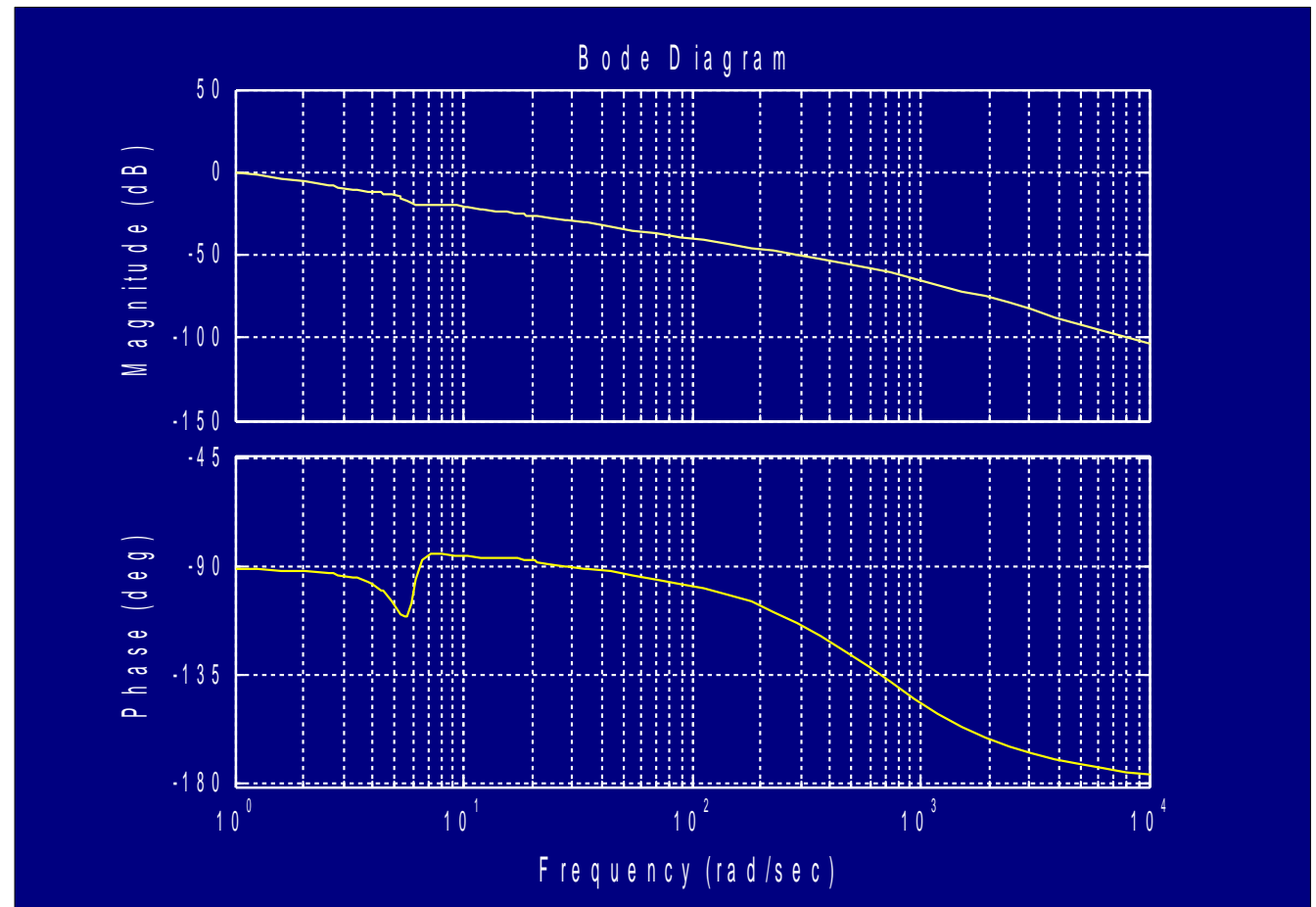
The anticipation parameter is tuned by means of a DF analysis techniques which suggest also the **introduction in-the-loop of a properly-tuned linear low-pass filter to enhance the system performance.**

# L5 – Contact Force Regulation

## Controller design

The integrator is introduced for anti-chattering purpose and the resulting relative degree is two

Harmonic response of the nominal plant with upper frame control and integrator

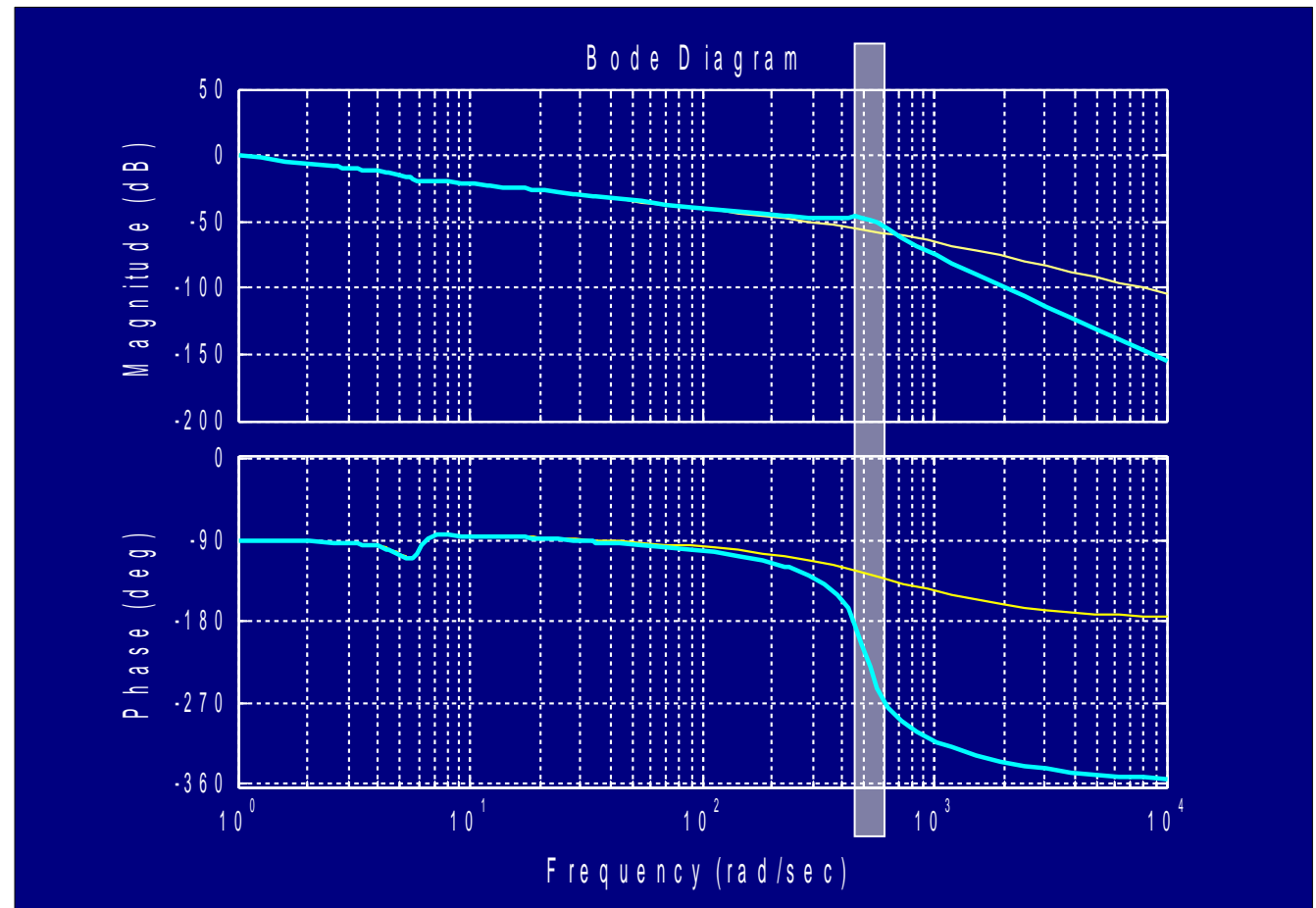


# L5 – Contact Force Regulation

## Controller design

The introduction of the resonant actuator causes the rise of large oscillations

Harmonic response of  
the nominal plant with  
upper frame control  
and integrator,  
plus the wire actuator



# L5 – Contact Force Regulation

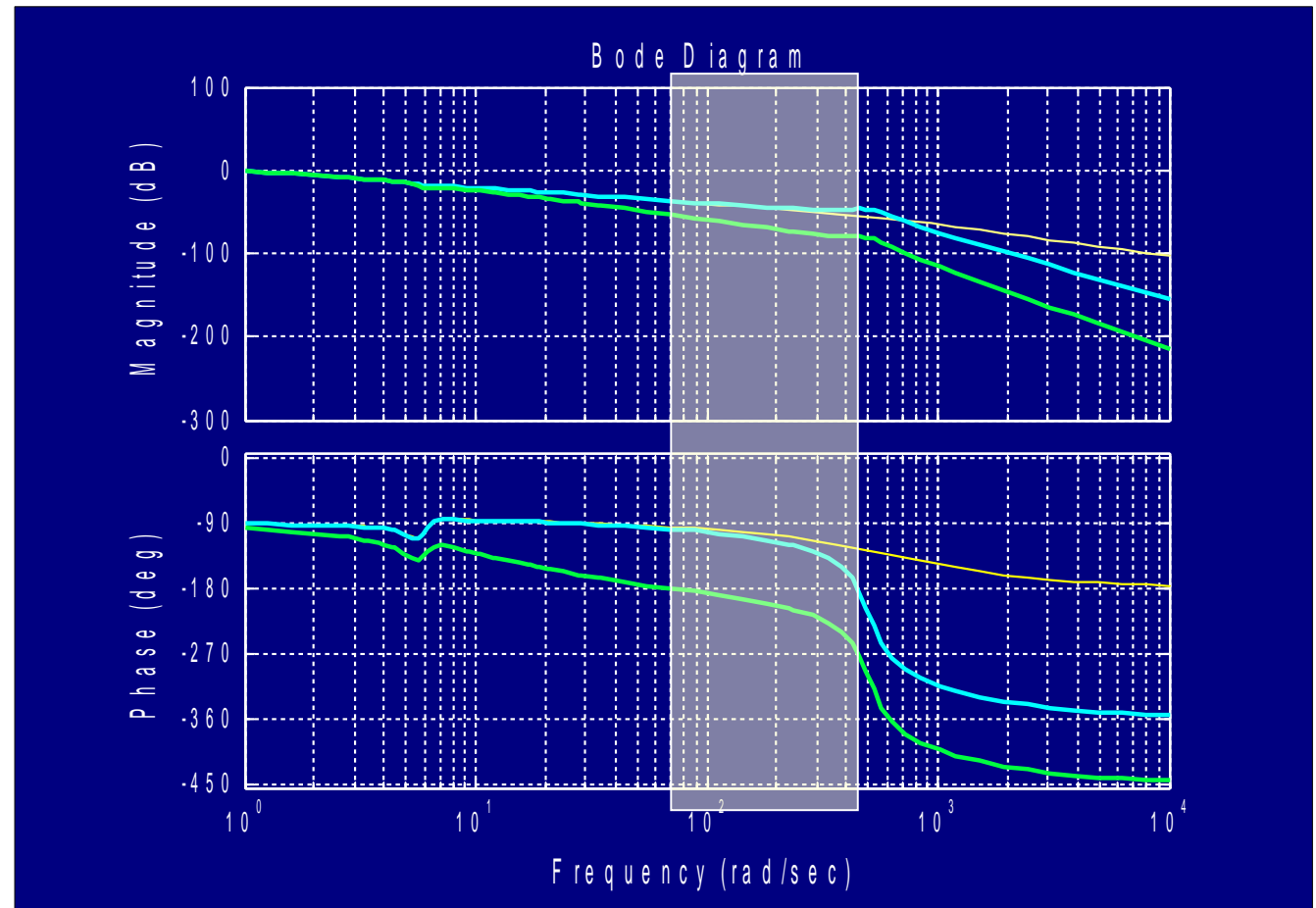
## Controller design

The pre-filter increases the relative degree of the input-output dynamics, but allows for choosing a suitable value of  $\beta$  such that oscillations are not too large

Harmonic response of the nominal plant with upper frame control and integrator,

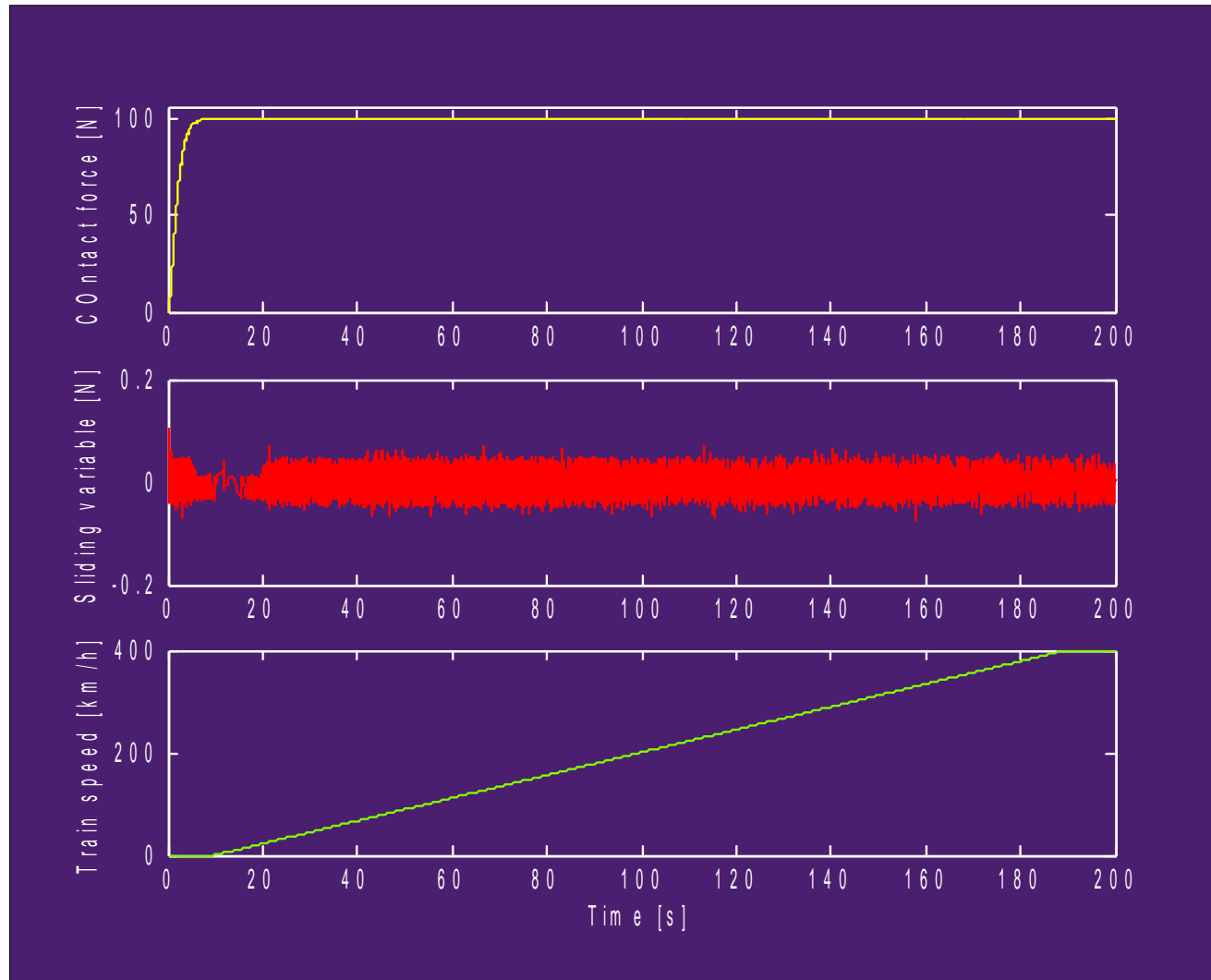
plus the wire actuator

And with the compensating pre-filter with  $\tau=0.1s$



# L5 – Contact Force Regulation

## Simulations



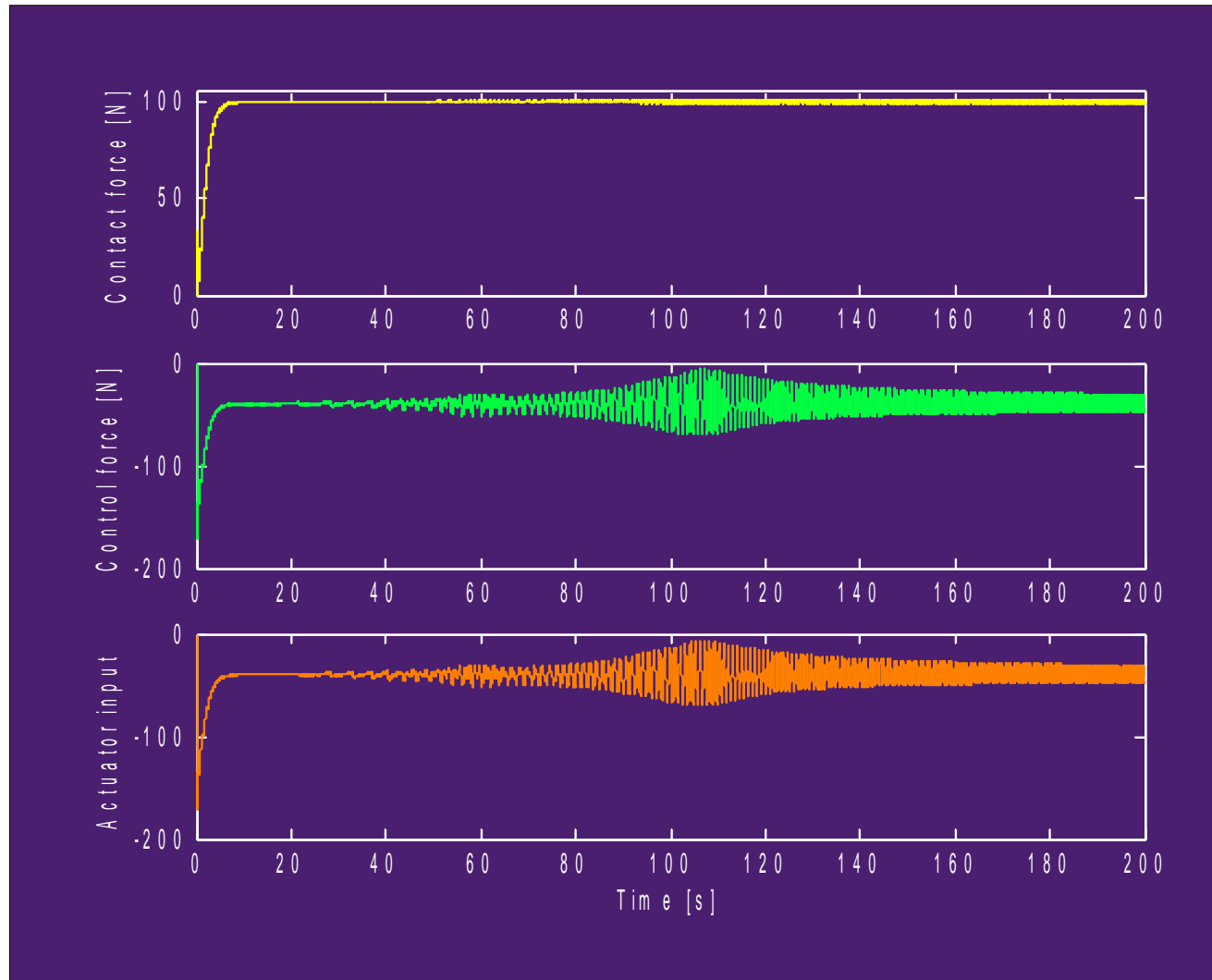
Upper frame control  
*No actuator dynamics*

$$U_M = 3000$$

$$\beta = 0.90$$

# L5 – Contact Force Regulation

## Simulations



Upper frame control

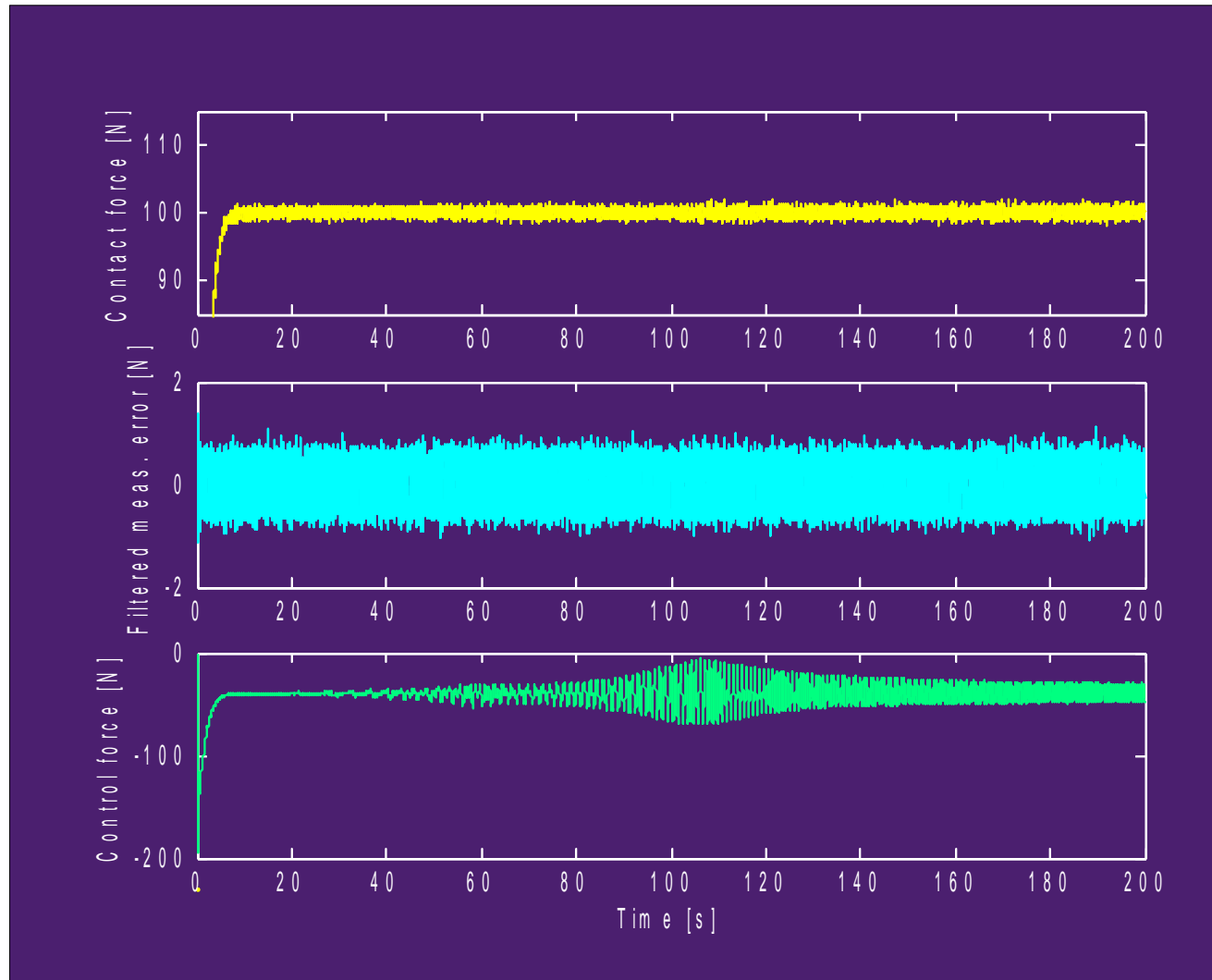
*Actuator*  
&  
*shaping pre-filter*  
 $\tau = 0.1$  s

$$U_M = 3000$$

$$\beta = 0.90$$

# L5 – Contact Force Regulation

## Simulations



Upper frame control  
*Actuator with  
measurement noise  $\pm 2N$*

&  
*shaping pre-filter  
 $\tau = 0.1$  s*

&  
*measurement filter  
 $\tau = 0.001$  s*

$$U_M = 3000$$

$$\beta = 0.90$$

# L5 – References

---

- Bartolini G., Ferrara A., Usai E., "Chattering avoidance by second-order sliding mode control", *IEEE Trans. Automatic Control*, 43, 241-246, 1998.
- Bartolini G., Ferrara A., Usai E., Utkin V.I., "On multi-input chattering-free second order sliding mode control", *IEEE Trans. Automatic Control*, 45, 1711-1717, 2000.
- Bartolini G., Pisano A., Usai E., Levant A., "On the robust stabilization of nonlinear uncertain systems with incomplete state availability", *J. of Dynamic Systems, Measurement and Control - Trans. ASME*, 122, 738-745, 2000.
- Bartolini G., Pisano A., Usai E., "Second-order sliding mode control of container cranes", *Automatica*, 38, 1783-1790, 2002.
- Bartolini G., Pisano A., Punta E., Usai E., "A survey of applications of second-order sliding mode control to mechanical systems", *International Journal of Control*, 76, pp. 875-892, 2003.
- Bartolini G., Pisano A., Usai E., "Output-feedback control of container cranes: a comparative analysis", *Asian Journal of Control*, 5, 578-593, 2003.

# L5 – References

---

- Boiko I., L. Fridman, R. Iriarte, A. Pisano and E. Usai, “Parameter tuning of second-order sliding mode controllers for linear plants with dynamic actuators”, *Automatica*, 42, 833-839, 2006.
- Compere M.D., Longoria R.G., “Combined DAE and Sliding Mode Control Methods for Simulation of Constrained Mechanical Systems”, *J. Dynamic Sys., Measurement, and Control–Trans. of ASME*, 122, 691–698, 2000.
- Pisano A., Usai E., “Output-Feedback Regulation of the Contact-Force in the High-Speed Train Pantographs”, *J. of Dynamic Systems, Measurement and Control - Trans. ASME*, 126, 82-87, 2004.
- Pisano A., Usai E., "Contact force regulation in wire-actuated pantographs via variable structure control and frequency-domain techniques", *International Journal of Control*, 81, 1747-1762, 2008.
- Rao S., Utkin V., Buss M., “Simulation of Constrained Dynamic Multibody Systems using Sliding Mode Control Theory”, *Proc. of the 10th Int. Workshop on Variable Structure Systems (VSS'08)*, pp. 7–12, Antalya, Turkey, 2008.